Supporting Information for:

Low-voltage solution-processed hybrid light-emitting transistors

Mujeeb Ullah Chaudhry[*1], Kornelius Tetzner[2], Yen-Hung Lin[4], Sungho Nam[4], Christopher Pearson [1], Chris Groves[1], Michael C. Petty[1], Thomas D. Anthopoulos[*2,3], Donal D. C. Bradley[*4,5]

[1] Department of Engineering, Durham University, Durham, DH1 3LE, United Kingdom
[2] Blackett Laboratory, Department of Physics and Centre for Plastic Electronics, Imperial College London, London SW7 2BW, United Kingdom
[3] Physical Science and Engineering Division, King Abdullah University of Science and Technology, Thuwal 23955, Saudi Arabia
[4] Department of Physics, University of Oxford, Oxford OX1 3PU, United Kingdom
[5] Department of Engineering Science, University of Oxford, Oxford OX1 3PJ, United Kingdom
* Correspondence: mujeeb.u.chaudhry@durham.ac.uk (MUC), thomas.anthopoulos@kaust.edu.sa (TA), donal.bradley@mpls.ox.ac.uk (DDCB)

Materials and Method

Materials and Methods:

Device Fabrication: The HLETs were fabricated with the 50 nm thick Al gate electrodes deposited on pre-cleaned glass substrates, by thermal evaporation through a shadow mask under high vacuum (~10^{-6} mbar). Next, a thin layer of native Al_2O_3 was grown by exposing the Al electrodes to ozone generated by a low-pressure mercury UV lamp operated at 5 mW/cm^2. The ZrO_x precursor solution was then spin-coated (3000 rpm, 30 s) on top under N_2, followed by a photochemical curing step in ambient air for 90 min using a metal halide lamp operated at 250 mW/cm^2. The In_2O_3 layer was subsequently grown by spin-coating (3000 rpm, 30 s) the precursor solution in air followed by thermal annealing at 300 °C also in air, repeated three times in order to increase thickness. The top ZnO layer was then deposited by spin-coating (3000 rpm, 30 s) the nanoparticle solution and thermal annealing at 300 °C in air.

Deposition of the ZrO_x dielectric layers used a precursor formulation as previously reported; [1] in brief, zirconium acetylacetonate ($Zr(C_5H_7O_2)_4$, 98%, Sigma-Aldrich) was dissolved under an inert gas atmosphere to a concentration of 0.15 M in N,N-dimethylformamide (DMF, C_3H_7NO, Sigma-Aldrich). An equal molar concentration of ethanolamine (EA, C_2H_7NO) (≥ 99% Sigma-Aldrich) was then added and the solution vigorously stirred at 90 °C for 1 h before use. In_2O_3/ZnO heterojunctions were deposited by spin-coating from solution, with In_2O_3 prepared using an indium nitrate hydrate precursor ($In(NO_3)3{\cdot}xH_2O$, 99.99%, Indium Corporation) dissolved in 2-methoxyethanol (99.8%, Sigma-Aldrich) at 30 mg/ml and ZnO nanoparticles (99.99%, Sigma-Aldrich) processed from 10 mg/mL aqueous ammonium hydroxide solution (NH_4OH, 50% v/v aqueous solution, Alfa Aesar).

HLET fabrication was completed using two shadow-masked evaporation steps, with intervening deposition of the emission layer polymer, to define complementary electron- and hole-injecting source (S) and, respectively, drain (D) contacts in a non-planar geometry

(**Figure 2(a)**). The 30 nm thickness electron-injecting Al S-electrode was first deposited directly on top of the In_2O_3/ZnO heterojunction. Then a 120 nm thickness layer of the emission polymer, Super Yellow [2], [3] (PDY-132 purchased from Merck), was spin-coated (2500 rpm, 30 s followed by 3000 rpm, 10 s), from toluene solution (7 mg/ml), over the whole structure. This was followed by annealing on a hotplate at 150 °C for 30 min and finally, the MoO_X/Au (10/20 nm) hole-injecting bilayer D-electrode was shadow-mask evaporated to complete the non-planar S-D geometry [2], [3]. The channel width and length of the resulting HLETs measured to be 1 mm and 100 μm, respectively. Thicknesses of the dielectric layers, semiconducting layers and electrode layers were measured using Dektak 150 stylus profilometer.

Electrical and Optical Characterization: The electrical and optical characteristics of the devices were tested within a nitrogen-filled glove box using an Agilent B2902A semiconductor parameter analyzer and a probe-station fitted with a calibrated photodiode positioned over the active region of the device according to our previously reported method [2], [3], [4]. Electroluminescence and Photoluminance spectra of the devices were measured using an Ocean-Optics USB4000-XR spectrometer equipped with optical fiber collection optics.

The luminance of the devices was obtained from the photocurrent measured with a photodiode calibrated against a super yellow OLED previously measured with a Konica Minolta LS-100 Luminance Meter, taking into account the relative emission areas. The HLET emission zone area was determined from the full width at half maximum intensity profile of the functioning devices measured with a digital camera attached to the probe station. External quantum efficiencies, EQEs, were calculated from the luminance, source-drain current and emission spectra of the devices under the assumption of Lambertian emission as reported previously [2], [3], [4].

The HLET charge carrier mobility was calculated from the electrical transfer characteristics in the saturation regime of operation, using the equation (1):

$$I_{DS} = \frac{W\,C_i}{2\times L}\,\mu\,(V_{GS} - V_{TH})^2 \qquad (1)$$

where I_{DS} is the experimentally measured drain-source current, W/L is the width-to-length ratio of the device channel, V_{GS} is the operating gate voltage and C_i is the geometric capacitance of the bilayer dielectric. The calculated mobility was further evaluated in relation to the non-ideality of the device characteristics and an effective mobility was calculated using the corresponding reliability factor in accordance with the method reported by *Choi et al* [5](as described in **Table S1**).

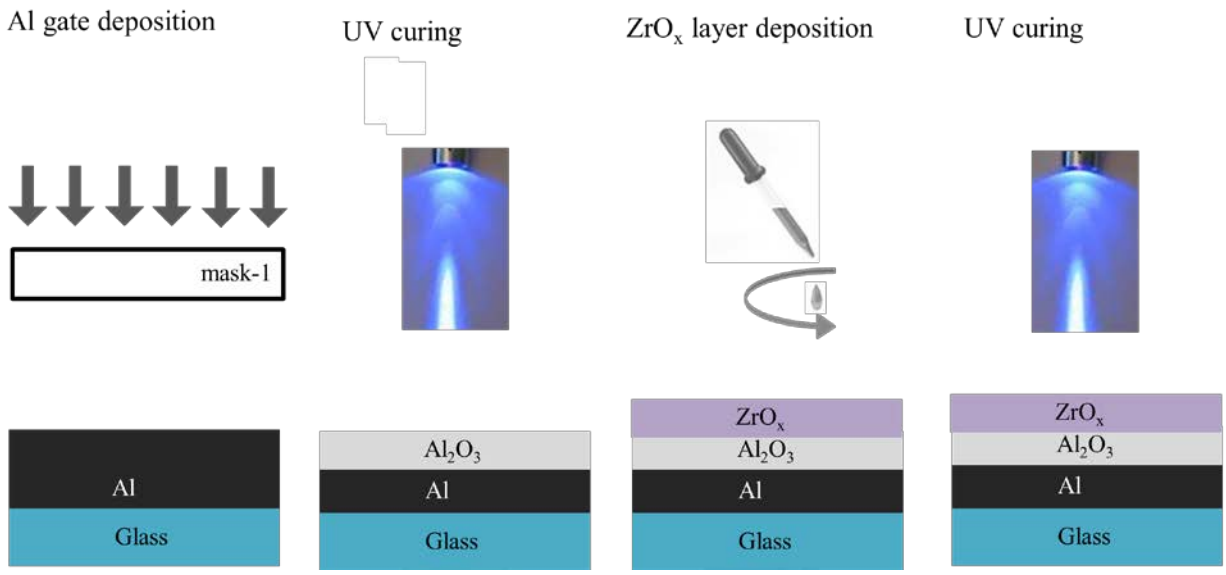

Figure S1: ***Device fabrication***: Deposition of gate electrode and processing dielectric layers.

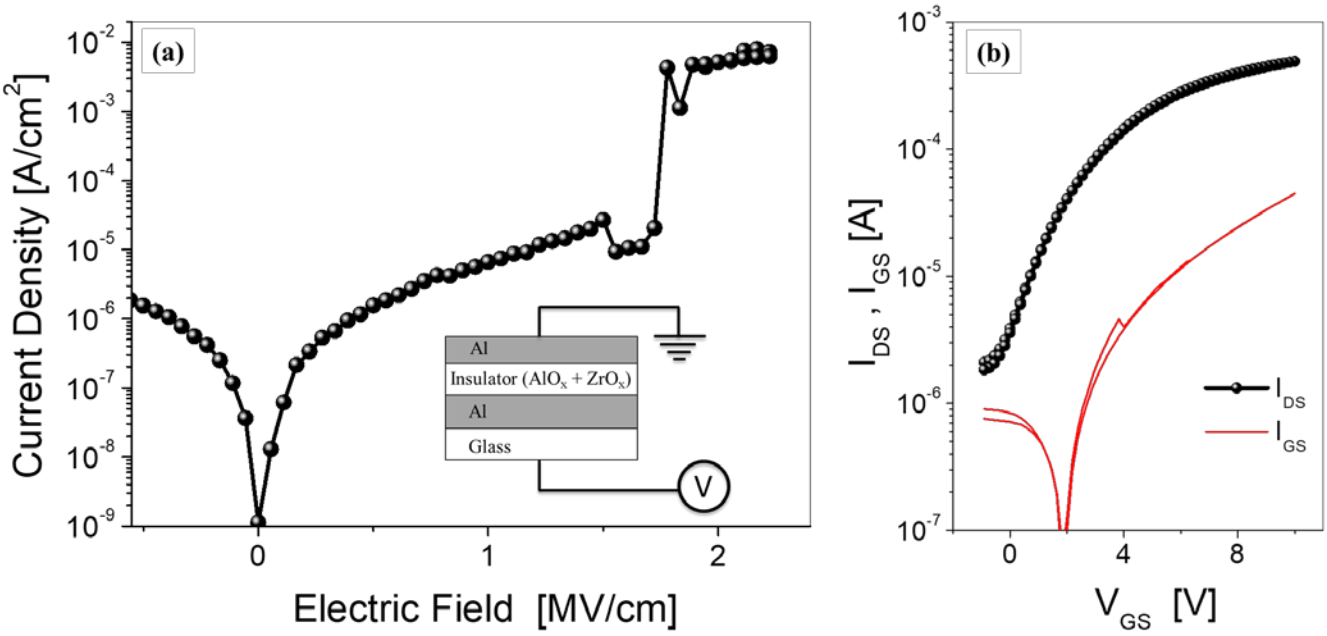

Figure S2: (a) Leakage current density versus applied electric field for the dielectric stack**.**

(b) Gate leakage current in HLET.

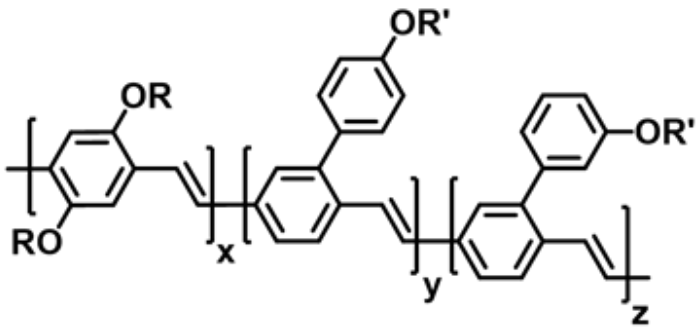

Super Yellow

Figure S3: Chemical structures of the light emitting polymer Super Yellow (SY).

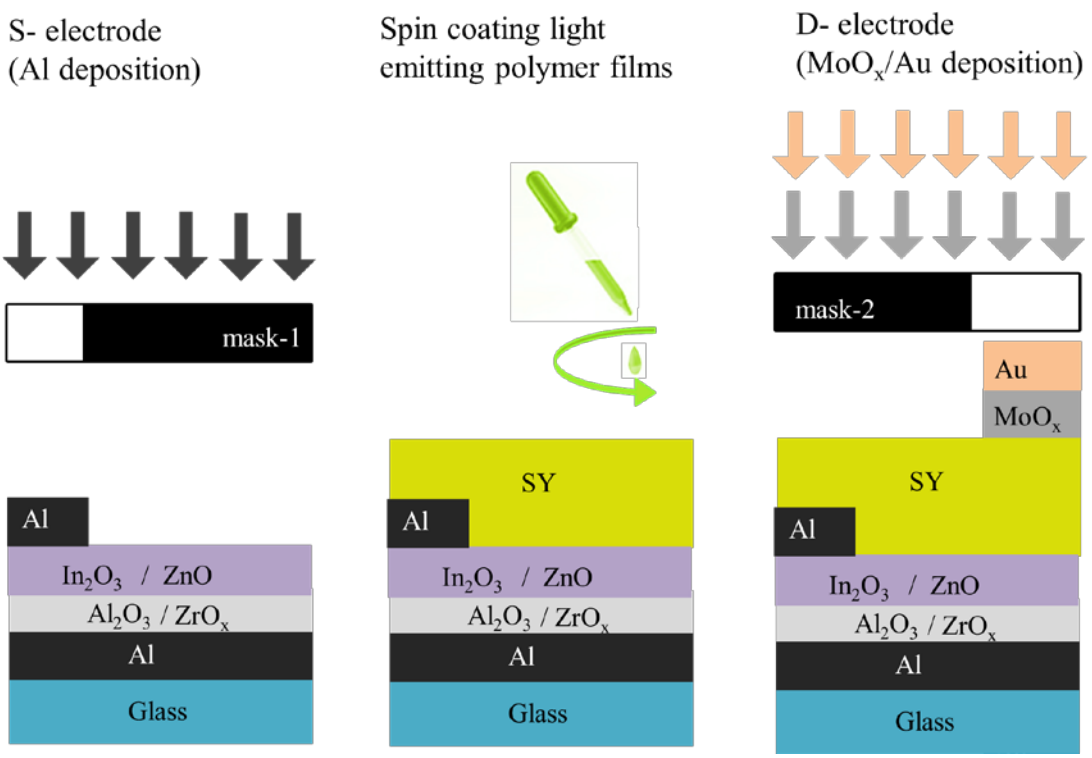

Figure S4: ***Device fabrication***: Deposition of electron injecting electrode, spin-coating of emissive layer and final evaporation of hole injecting electrode.

Mobility calculation and reliability factor:

The reliability factor [5], r, in the FET mobility measurements describes deviation of the behavior of reported FETs from the simple linear increase of conductivity with gate voltage (assuming a constant mobility and negligible threshold voltage). Reliability factor, thus defined as the ratio of the experimentally determined FET channel conductivity at the maximum applied gate voltage to the FET channel conductivity expected in an ideal FET at the same maximum gate voltage (using calculated mobility μ and same device parameters). In the saturation regime, reliability factor, r_{sat} is calculated as:

$$r_{sat} = \left[\frac{\sqrt{|I_{SD}|^{max}} - \sqrt{|I_{SD}|^{0}}}{|V_{GS}|^{max}}\right]^2 \Bigg/ \left[\frac{WC_i}{2L}\,\mu_{sat}\right]_{calculate} = \left[\frac{\sqrt{|I_{SD}|^{max}} - \sqrt{|I_{SD}|^{0}}}{|V_{GS}|^{max}}\right]^2 \Bigg/ \left[\frac{\partial\sqrt{|I_{SD}|}}{V_{GS}}\right]^2_{calculated} \quad (1)$$

Here, μ_{sat} is the experimentally calculated mobility, L, W and C_i are the channel length, channel width and geometric capacitance respectively. $|I_{SD}|^{max}$ is the experimentally determined source-drain current at $|V_{GS}|^{max}$, and $|I_{SD}|^{0}$ is the source-drain current at $V_{GS} = 0$.

The effective mobility 'μ_{eff}' is the claimed mobility value at the reliability factor of 100% and is calculated (according to Reference 1) as:

$$\mu_{eff} = r \times \mu_{claimed}$$

Table S1:

μ_{sat} ($cm^2 V^{-1} s^{-1}$)		**μ_{eff}** ($cm^2 V^{-1} s^{-1}$)
$\mu_{calculated}$	**r %**	
22	195 %	43

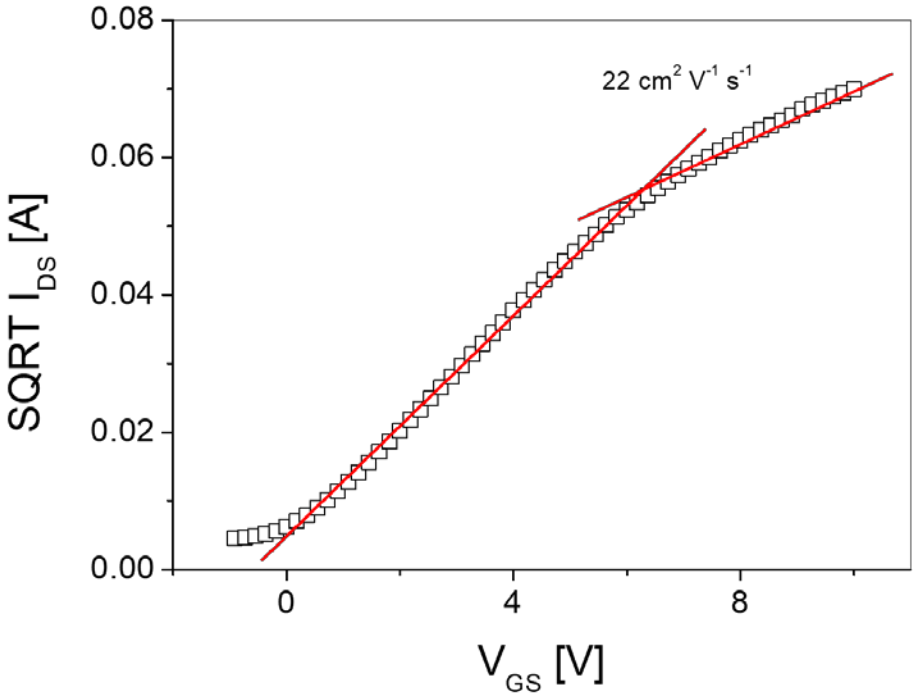

Figure S5: Double slope, linear fit to a 'square root of (I_{DS}) *vs* V_{GS}' plot for one of our HLET devices. We have calculated mobility from a linear fit at high gate voltages. Calculation for a reliability factor of 195% yields an effective mobility of 43 $cm^2\ V^{-1}\ s^{-1}$, which we consider to be the more accurate value (see recent literature reports for further discussion).[1],[6],[7]

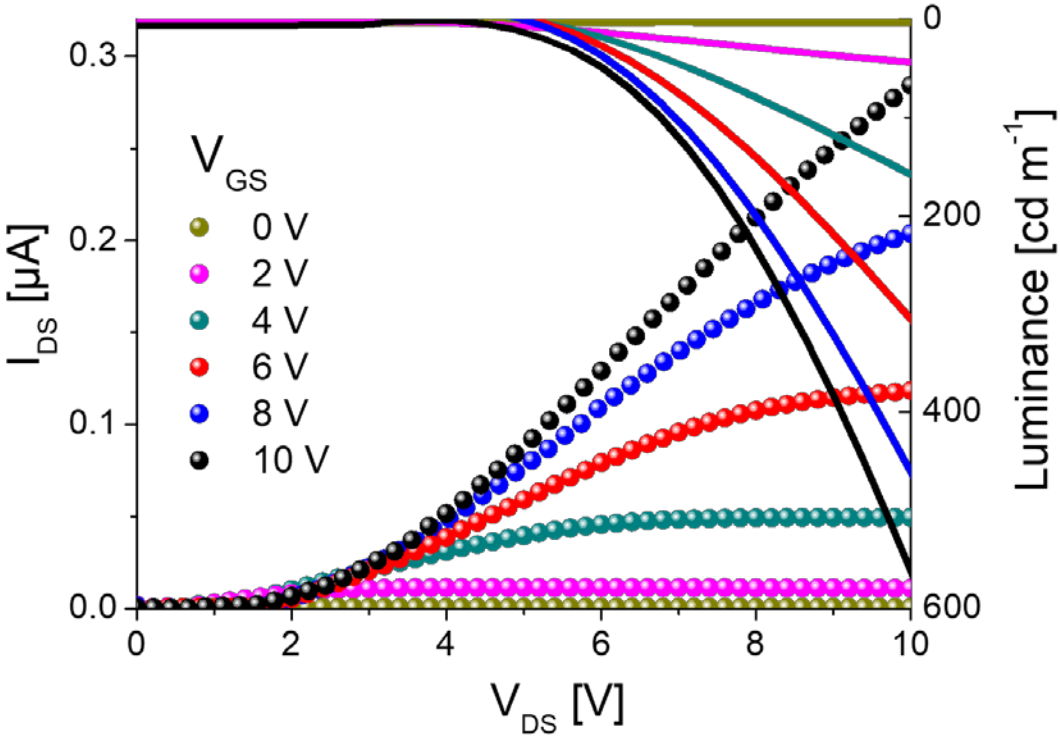

Figure S6: Electrical (I_{DS}, circles) and optical (Luminance, solid lines, increasing down) device output characteristics**.**

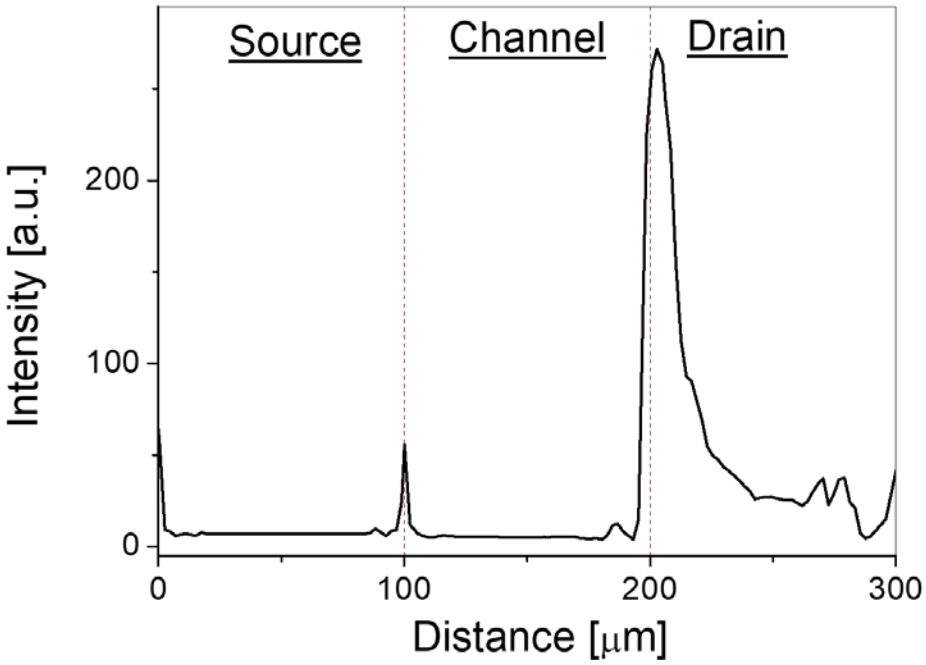

Figure S7: Microscopic image intensity profile of the light emission from the HLET channel and electrodes.

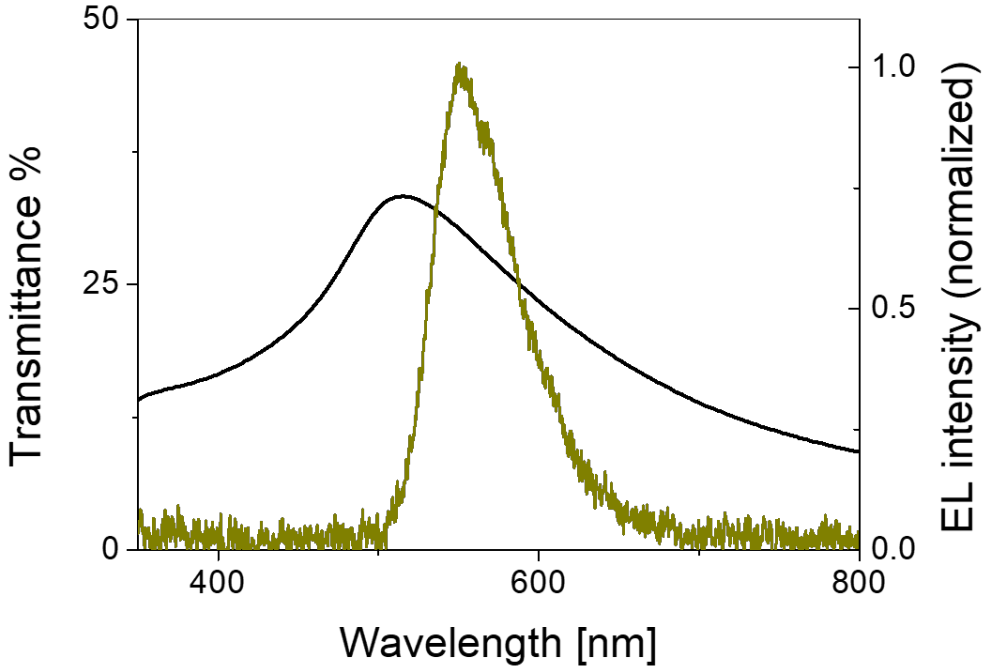

Figure S8: Transmittance of the hole injecting (MoO_x/Au) electrode and electroluminance intensity of HLET.

Table S2: Comparison of the HLET performance of this work with literature

A comparison of the electrical and optical characteristics demonstrated in this study with those reported to date for hybrid light emitting transistors (HLETs).

REFERENCE	**This Study**	**Muhieddine et al [8]**	**Muhieddine et al [9]**	**Yamada et al [10]**	**Yamada et al [10]**	**Nakanotani et al [11]**
Device Type	Bilayer	Bilayer	Bilayer	Bilayer	Blended Layer	Bilayer
Oxide	Solution Processed In_2O_3/ZnO	Solution Processed ZTO	Solution Processed ZTO	Evaporated AZO Floating Gate	Solution Processed ZTO	Sputtered IZO
Emissive Material	Solution Processed Super Yellow	Solution Processed Super Yellow	Solution Processed Super Yellow	Solution Processed BP3T	Part Sublimed Tetracene	Evaporated Tetracene
Gate / Dielectric	Al / Al_2O_3 / ZrO_x	Si/SiNx	Si/SiNx	Si/SiO_2	Si/SiO_2	Si/SiO_2
Max. operating voltage (V)	10	100	100	100	100	100
Mobility ($cm^2 V^{-1} s^{-1}$)	22	4.2	1.62	10^{-2} - 10^{-3}	$8.1x10^{-1}$	13.8
ON/OFF Ratio	~ 10^3	~ 10^4	~ 10^5	Not Reported	Not Reported	Not Reported
Luminance ($cd\ m^{-2}$)	700	413	1330	Not Reported	Not Reported	Not Reported
EQE (%)	0.02	0.0018	0.087	Not Reported	Not Reported	$6.7x10^{-5}$

References for Supporting Information:

[1] Park, Y. M.; Desai A.; Salleo, A. Solution-Processable Zirconium Oxide Gate Dielectrics for Flexible Organic Field Effect Transistors Operated at Low Voltages. *Chem.Mater*. **2013**, 25, 2571.

[2] Ullah, M.; Tandy, K.; Yambem, S. D.; Aljada, M.; Burn, P. L.; Meredith, P.; Namdas, E. B. Simultaneous Enhancement of Brightness, Efficiency, and Switching in RGB Organic Light Emitting Transistors. *Adv. Mater*. **2013**, 25, 6213.

[3] Ullah, M.; Armin, A.; Tandy, K.; Yambem, S. D.; Burn, P. L.; Meredith, P.; Namdas, E. B. Defining the Light Emitting Area for Displays in the Unipolar Regime of Highly Efficient lLight Emitting Transistors. *Sci. Rep*. **2015**, 5, 8818.

[4] Chaudhry, M. U.; Muhieddine, K.; Wawrzinek, R.; Li, J.; Lo, S-C.; Namdas, E. B. Nano-Alignment in Semiconducting Polymer Films: A Path to Achieve High Current Density and Brightness in Organic Light Emitting Transistors. *ACS Photonics*. **2018**, doi: 10.1021/acsphotonics.8b00011.

[5] Choi, H. H.; Cho, K; Frisbie, C. D.; Sirringhaus, H.; Podzorov, V. Critical Assessment of Charge Mobility Extraction in FETs. *Nat. Mater*. **2018**, 17, 2-7.

[6] a) Bittle, E. G.; Basham, J. I.; Jackson, T. N.; Jurchescu, O. D.; Gundlach, D. J. Mobility Overestimation Due to Gated Contacts in Organic Field-Effect Transistors. *Nat. Comm*. 7, 10908, (2016); b) McCulloch, I.; Salleo, A.; Chabinyc, M. ORGANIC DEVICES. Avoid the Kinks When Measuring Mobility. *Science*. **2016**, 352-6293, 1521.

[7] Uemura, T.; Rolin, C.; Ke, T. H.; Fesenko, P.; Genoe, J.; Hermans, P.; Takeya, J. On the Extraction of Charge Carrier Mobility in High-Mobility Organic Transistors. *Adv. Mater*. **2015**, 28, 151–155.

[8] Muhieddine, K.; Ullah, M.; Pal, B. N.; Burn, P.; Namdas, E. B. All Solution-Processed, Hybrid Light Emitting Field-Effect Transistors. *Adv. Mater.* **2014**, 26, 37, 6410.

[9] Muhieddine, K;. Ullah, M.; Maasoumi, F.; Burn, P. L.; Namdas, E. B. Hybrid Area Emitting Transistors: Solution Processable and with High Aperture Ratios. *Adv. Mater*. **2015**, 27, 42, 6677.

[10] Yamada, K; Yamao, T.; Hotta, S. Light-Emitting Field-Effect Transistors Having Combined Organic Semiconductor and Metal Oxide Layers.*Adv. Mater.* **2013**, 25, pp. 2860-2866.

[11] Nakanotani, H.; Yahiro, M.; Adachia, C. Ambipolar Field-Effect Transistor Based on Organic-Inorganic Hybrid Structure. *Appl. Phys. Lett.* **2007**, 90, 262104.